

EFFECT OF TEST TEMPERATURE AND STRAIN RATE ON THE TENSILE PROPERTIES OF HIGH-STRENGTH, HIGH-CONDUCTIVITY COPPER ALLOYS — S. J. Zinkle and W. S. Eatherly (Oak Ridge National Laboratory)

OBJECTIVE

The objective of this report is to summarize recent tensile and electrical resistivity measurements on several different unirradiated commercial high-strength, high-conductivity copper alloys that are being considered for the divertor structure and first wall heat sink in ITER.

SUMMARY

The unirradiated tensile properties of wrought GlidCop AL25 (ITER grade zero, IG0), solutionized and aged CuCrZr, and cold-worked and aged and solutionized and aged Hycon 3HP™ CuNiBe have been measured over the temperature range of 20-500°C at strain rates between $4 \times 10^{-4} \text{ s}^{-1}$ and 0.06 s^{-1} . The measured room temperature electrical conductivity ranged from 64 to 90% IACS for the different alloys. All of the alloys were relatively insensitive to strain rate at room temperature, but the strain rate sensitivity of GlidCop AL25 increased significantly with increasing temperature. The CuNiBe alloys exhibited the best combination of high strength and high conductivity at room temperature. The strength of CuNiBe decreased slowly with increasing temperature. However, the ductility of CuNiBe decreased rapidly with increasing temperature due to localized deformation near grain boundaries, making these alloy heats unsuitable for typical structural applications above 300°C. The strength and uniform elongation of GlidCop AL25 decreased significantly with increasing temperature at a strain rate of $1 \times 10^{-3} \text{ s}^{-1}$, whereas the total elongation was independent of test temperature. The strength and ductility of CuCrZr decreased slowly with increasing temperature.

PROGRESS AND STATUS

Introduction

High-strength, high-conductivity copper alloys have been selected for first wall heat sink and divertor structural applications in the proposed International Thermonuclear Experimental Reactor (ITER) [1,2]. The divertor structure poses a particularly challenging operating environment, where good mechanical properties (strength, fatigue, etc.) and high thermal conductivity are required. The proposed operating temperatures for the divertor structure and first wall heat sink range from ~100 to 350°C. Three different copper alloys are under consideration for fusion energy high heat flux applications, namely dispersion strengthened copper (Cu-Al₂O₃), CuCrZr and CuNiBe.

The purpose of the present report is to summarize recent tensile measurements performed on unirradiated specimens of these three alloys in ITER-relevant thermomechanical conditions. The reference thermomechanical conditions for the proposed ITER applications are as-wrought for the dispersion-strengthened copper, and solutionized and aged for the CuCrZr and CuNiBe alloys. At the present time, there are no known tensile data for solutionized and aged CuCrZr or CuNiBe over the temperature range of 100-350°C which is of interest for ITER. Tensile measurements were performed at temperatures between 20 and 500°C and at strain rates between 4×10^{-4} and 0.06 s^{-1} in order to identify key trends in the deformation behavior. Room temperature electrical resistivity measurements were also performed in order to obtain thermal stress figures of merit for the different alloys.

Experimental Procedure

Four different copper alloy heats were selected for the tensile measurements. The dispersion strengthened (DS) copper specimens were cut from a 2.5 cm thick plate of GlidCop AL25 DS copper produced by SCM Metal Products (now known as OMG Americas), which was fabricated according to

"ITER grade 0" [3] specifications (heat #C-8064). This alloy contains 0.25 wt.% Al in the form of finely dispersed aluminum oxide particles. The copper cladding on the plate surface was machined off prior to specimen fabrication. The tensile axis of the specimens were oriented along the longitudinal direction of the wrought plate. The Cu-0.65%Cr-0.10%Zr specimens were obtained from a 2 cm thick plate that was originally fabricated under the trade name of Elbrodur G by KM-Kabelmetal, Osnabrück, Germany as an F37 (cold-worked and aged) temper, heat #AN4946. A 2 × 3 × 5 cm piece from this plate was solution annealed in flowing argon for 1 hour at 980°C, water quenched, then aged in flowing helium at 475°C for 2 hours (furnace cool) at ORNL, in accordance with the draft ITER heat treatment specifications. Two different Hycon 3HP™ Cu-2%Ni-0.35%Be heats produced as 2.5 cm thick plates by Brush-Wellman were investigated. A cold-worked and aged plate (longitudinal orientation, heat #33667Y1) was fabricated to produce maximum strength while still providing reasonable conductivity [4], and is referred to in the following as HT1 temper. In addition, a solutionized and aged (AT temper) plate of Hycon 3HP™ CuNiBe was obtained by heat treating a cold-worked and aged plate (heat #46546, designated HT2 in the following) at Brush-Wellman. Miniature SS-3 sheet tensile specimens with nominal gage dimensions 0.76 mm × 1.5 mm × 7.6 mm were electro-discharge machined from all four plates and tested without any subsequent heat treatment.

The tensile properties of the SS-3 sheet tensile specimens were determined at temperatures between 20 and 500°C at crosshead speeds ranging from 0.003 to 0.42 mm/s, which corresponds to initial strain rates of 3.9×10^{-4} to 0.056 s^{-1} in the gage region. The room temperature tests were performed in air, and the elevated temperature tests were performed in vacuum (10^{-6} to 10^{-5} torr). The specimens were held at the test temperature for 0.25 h prior to the start of each tensile test. One or two specimens were typically tested in an Instron servohydraulic machine for each experimental condition. The tensile properties were determined from graphical analysis of the chart recorder curves. A plastic deformation offset of 0.2% was used for measuring the yield strength.

Four-point probe electrical resistivity measurements were performed at room temperature on a minimum of 5 different SS-3 sheet tensile specimens for each of the alloys, using procedures summarized elsewhere [4]. The temperature was recorded for each measurement and the resistivity data were corrected to a reference temperature of 20°C using the copper resistivity temperature coefficient of $dp/dT = 6.7 \times 10^{-11} \text{ } \Omega\text{-m/K}$. Nonuniformities in the width and thickness in the specimen gage region caused the typical experimental uncertainty of individual resistivity measurements to be $\pm 0.5\%$.

Results

Table 1 summarizes the results of the room temperature electrical resistivity measurements. The relation $17.241 \text{ n}\Omega\text{-m}=100\%$ IACS (international annealed copper standard) was used to convert the resistivity measurements to the familiar normalized conductivity scale. Previously reported results for the HT2 temper heat of Hycon 3HP™ CuNiBe [4] are also included in Table 1 for comparison. GlidCop Al25 exhibited the highest conductivity, followed by CuCrZr and CuNiBe. The measured values are in reasonable agreement with conductivities reported by the vendors. It is interesting to note that the AT heat treatment of the HT2 CuNiBe plate caused a reduction in the electrical conductivity.

The tensile properties obtained in the present study are summarized in Table 2. Additional data on the HT1 and HT2 heats of Hycon 3HP™ CuNiBe have been reported previously [4] for temperatures between 20 and 500°C at a strain rate of $1.1 \times 10^3 \text{ s}^{-1}$. Figure 1 compares the 0.2% yield strength of the 4 different materials as a function of test temperature. All of the data in these two plots were obtained at an initial strain rate of $2.2 \times 10^3 \text{ s}^{-1}$ with the exception of the CuNiBe HT1 (heat #33667) data, which was obtained at a strain rate of $1.1 \times 10^3 \text{ s}^{-1}$. The CuCrZr and GlidCop Al25 alloys exhibited similar yield strengths over the temperature range of 20-300°C, whereas both the AT and HT1 CuNiBe heats had much higher yield strengths. The yield strength of the CuNiBe AT temper was about 50 MPa lower than the parent HT2 temper [4] at room temperature. The AT and HT1 tempers had comparable strengths at temperatures $\geq 300^\circ\text{C}$. It is interesting to note that the strength of CuCrZr determined from these short term tensile tests was higher than that of GlidCop Al25 at 500°C. The

Table 1. Comparison of vendor data with electrical conductivities measured in the present study

Alloy	Nominal conductivity	Meas. resistivity at 20°C	Electrical conductivity
GlidCop Al25 (IGO)	86% IACS [5]	19.12 nΩ-m	90% IACS
CuCrZr (ITER SAA)	~80-83% IACS	20.67 nΩ-m	83% IACS
Hycon 3HP CuNiBe (AT)	65% IACS [5]	26.78 nΩ-m	64% IACS
Hycon 3HP CuNiBe (HT1)*	68% IACS [4]	26.27 nΩ-m	66% IACS
Hycon 3HP CuNiBe (HT2)*	74% IACS [4]	24.05 nΩ-m	72% IACS

*HT1= Hycon 3HP™ heat #33667 ; HT2= Hycon 3HP™ heat #46546

Table 2. Summary of tensile data from the present study (asterisks denote duplicate specimen averages)

	Temperature	σ_y (MPa)	UTS (MPa)	e_u (%)	e_{tot} (%)
GlidCop Al25 (IGO)					
$3.9 \times 10^{-4} \text{ s}^{-1}$	20°C	313	377	10.0	20.8
	200°C	263	314	11.9	35.0
	300°C	200	250	3.1	24.6
	500°C	75	104	30.3	68.0
$2.2 \times 10^{-3} \text{ s}^{-1}$	20°C	324	411	13.4	24.0
	200°C	287	333	8.4	26.4
	300°C	229	272	5.5	28.3
	500°C	92	134	4.0	45.0
0.056 s^{-1}	20°C	335	435	13.5	21.7
	200°C	292	359	10.7	27.2
	300°C	282	306	7.8	29.2
CuCrZr (ITER SAA)					
$3.9 \times 10^{-4} \text{ s}^{-1}$	20°C	300	407	15.4	23.2
	200°C	276*	359*	24.3*	42.2*
	300°C	253	313	12.0	23.0
$2.2 \times 10^{-3} \text{ s}^{-1}$	20°C	316	414	16.2	24.2
	200°C	280*	357*	13.8*	23.2*
	300°C	275*	332*	12.0*	23.7*
	500°C	197	223	11.4	30.0
0.056 s^{-1}	20°C	322	433	20.7	27.8
	300°C	264	330	14.3	24.3
CuNiBe (AT)					
$3.9 \times 10^{-4} \text{ s}^{-1}$	20°C	569	720	15.9	18.6
	200°C	550	672	14.9	16.0
	300°C	510	581	1.9	1.9
$2.2 \times 10^{-3} \text{ s}^{-1}$	20°C	564	723	15.3	18.0
	200°C	553	669	11.6	13.4
	300°C	545	595	2.6	2.8
	400°C	520	543	0.8	0.9
	500°C	(>420)**	—**	—**	—**
0.056 s^{-1}	20°C	596	728	17.5	18.5
	200°C	570	688	13.5	13.6
	300°C	543	621	6.0	6.0
	400°C	523	567	1.2	1.3
CuNiBe 33667 (HT1)					
$3.9 \times 10^{-4} \text{ s}^{-1}$	20°C	700	787	6.7	9.0
	300°C	649	712	2.1	3.2
$2.2 \times 10^{-3} \text{ s}^{-1}$	20°C	732	817	6.7	10.2
	20°C	728	769	9.8	13.3
0.056 s^{-1}	20°C	728	769	9.8	13.3
	300°C	681	713	5.0	6.8

**broke in specimen grip pin hole; 2 different samples

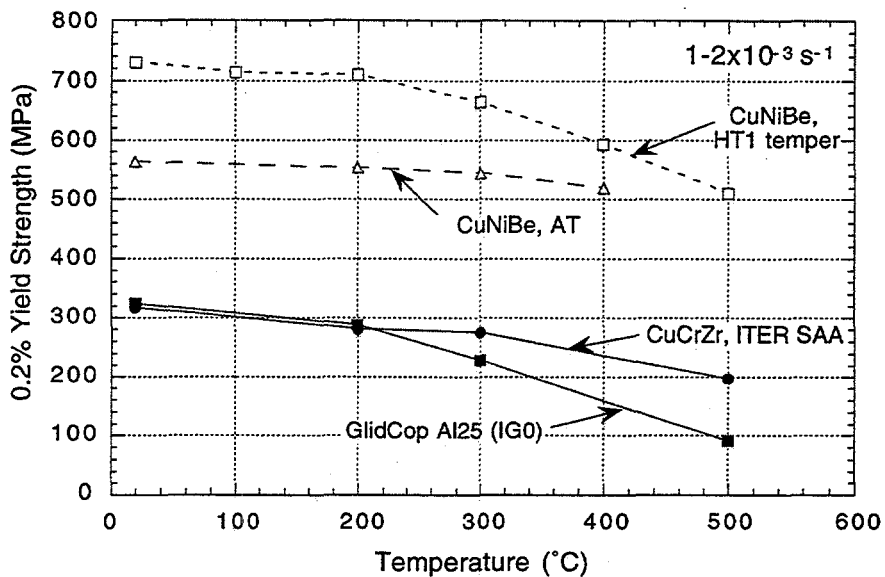


Fig. 1. Comparison of the temperature-dependent yield strengths of the four high-strength, high-conductivity copper alloy heats.

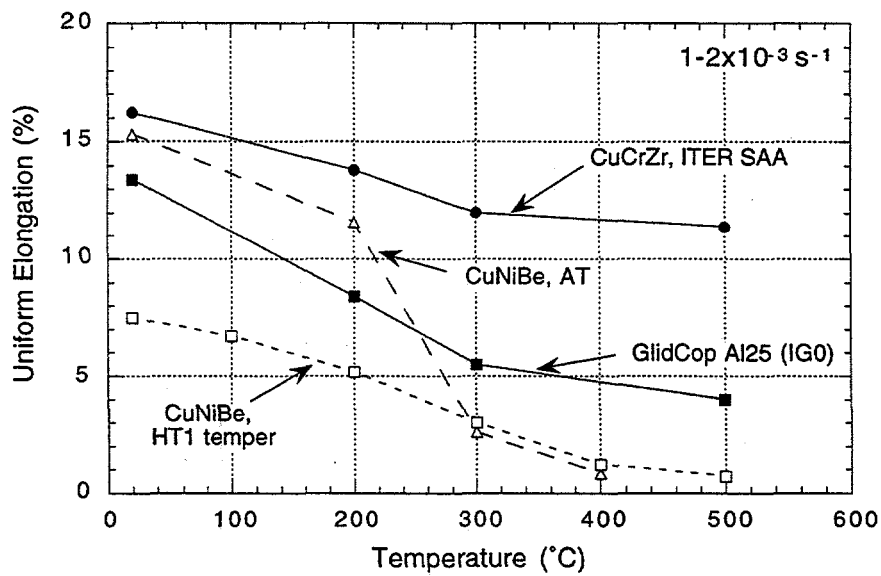


Fig. 2. Comparison of the temperature-dependent uniform elongations of the four high-strength, high-conductivity copper alloy heats.

strength of GlidCop dropped off more rapidly with increasing test temperature than any of the other alloys. For example, the measured yield strength for GlidCop Al25 at 300°C was 71% of its room temperature value. The corresponding 300°C yield strength ratios for the other alloys were 87% for CuCrZr and 91-97% for the two CuNiBe heats.

Figure 2 shows the uniform elongations as a function of temperature for the 4 different materials at a strain rate of 1 to $2 \times 10^{-3} \text{ s}^{-1}$. All of the materials tested exhibited good ductility at room temperature. However, the behavior at elevated temperature was significantly different for each of the different alloys. The uniform elongation of CuCrZr decreased only slightly from ~16% at room temperature to ~12% at 500°C. In contrast, the uniform elongations of GlidCop and both CuNiBe heats decreased strongly with increasing test temperature. The uniform elongation of GlidCop Al25 decreased from ~13% at room temperature to ~4% at 500°C. The GlidCop Al25 total elongation remained high at all temperatures, with values between 25 and 45% at temperatures of 300-500°C (Table 1). The GlidCop elongation data indicate that necking (localized deformation) occurred at lower deformation levels with increasing test temperature, but high ductility was present in the necked region at all temperatures. The most severe elevated temperature embrittlement behavior occurred in the CuNiBe alloys, where the uniform elongation was reduced to <5% at a temperature of ~250°C. The decrease in uniform elongation in the CuNiBe alloys at elevated temperatures was accompanied by a pronounced decrease in the total elongation as well (cf. Table 2). Scanning electron microscopy of the fracture surfaces showed a transition from ductile transgranular failure at room temperature to intergranular failure (with localized ductile deformation) at elevated temperatures.

Figure 3 shows the effect of strain rate ($\dot{\epsilon}$) on the measured yield strengths (σ_y) of the four materials tested at room temperature and 300°C. In general, all of the materials exhibited a very weak strain rate dependence, with a strain rate sensitivity parameter [6,7] of $m \sim 0.01$, where $\sigma_y = C \dot{\epsilon}^m$ and C is a constant. However, the strain rate sensitivity of GlidCop Al25 increased with increasing test temperature. A value of $m=0.07$ was measured at 300°C, which agrees well with another recent tensile test measurement on this alloy [8]. Previous work on GlidCop Al15 reported that $m \sim 0.1$ for test temperatures of 400-650°C [9]. Due to the increased strain rate sensitivity of GlidCop at elevated temperatures, it can be seen in Fig. 3 that the yield strength of GlidCop Al25 at 300°C is comparable or greater than that of CuCrZr at a strain rate of 0.06 s^{-1} , but is 50 MPa weaker than CuCrZr at a strain rate of $4 \times 10^{-4} \text{ s}^{-1}$. A qualitatively similar strain rate dependence was also observed for the ultimate tensile strengths of the 4 materials. The measured strain rate parameters obtained from the ultimate tensile strength data were $m \leq 0.01$ for all alloys except for GlidCop Al25, which exhibited $m=0.03$ and $m=0.04$ at room temperature and 300°C, respectively.

The uniform elongations of the alloys were somewhat more sensitive to strain rate than the yield and ultimate strengths. In all cases, the uniform elongation increased with increasing strain rate. The value of the uniform elongation strain rate exponent was $m' \sim 0.05$ for all of the alloys at room temperature. A similar value was also obtained for CuCrZr tested at 300°C, whereas the value of m' increased to ~0.2 for the GlidCop and CuNiBe alloys tested at 300°C. The total elongation was not significantly affected by strain rate, with the notable exception of the CuNiBe specimens tested at elevated temperatures which exhibited an increase in total elongation with increasing strain rate.

Indications of an approach to superplastic deformation behavior were observed in the GlidCop Al25 and Kabelmetal CuCrZr specimens under certain combinations of strain rate and test temperature (Table 2). The GlidCop specimens exhibited a dramatic increase in uniform and total elongation at 500°C for the slowest strain rate investigated in this study, $4 \times 10^{-4} \text{ s}^{-1}$. A somewhat less pronounced increase in ductility was observed for CuCrZr specimens tensile tested at 200°C at $4 \times 10^{-4} \text{ s}^{-1}$. Further work is needed to determine if even higher levels of elongation can be achieved in these alloys through a suitable combination of strain rate and test temperature.

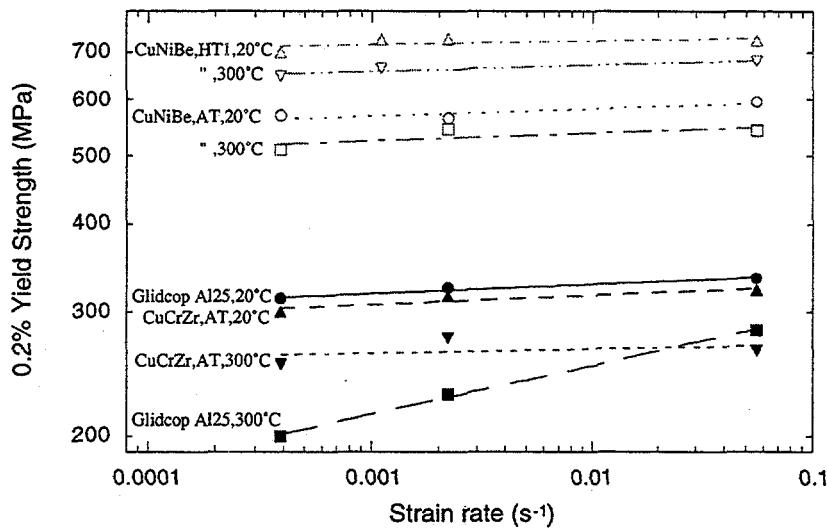


Fig. 3. Effect of strain rate on the yield strengths of the four high-strength, high-conductivity copper alloy heats at room temperature and 300°C.

Discussion

Table 3 compares the thermal stress figures of merit, $M = \sigma_y k_{th} (1-\nu) / \alpha E$, at room temperature and 300°C for the four materials tested in this study. The M values were calculated using the temperature-dependent pure copper data [1] for Young's modulus (E), Poisson's ratio (ν) and the coefficient of thermal expansion (α), and by utilizing the Wiedemann-Franz relation to convert the electrical conductivity measurements to thermal conductivity (k_{th}). The yield stress (σ_y) measured at a strain rate near $1 \times 10^{-3} \text{ s}^{-1}$ was used for the calculations. Table 3 also contains data for the HT2 temper of CuNiBe, which was the parent material for the AT specimens. The calculated thermal stress figures of merit decrease with increasing temperature for all of the alloys, mainly due to the decrease in yield strength. Small decreases in thermal conductivity and an increase in the Poisson's ratio also act to decrease the value of M at elevated temperatures, but they are partially balanced by a small decrease in Young's modulus [1]. The CuNiBe alloys exhibit the highest values for the thermal stress figure of merit over the temperature range of interest for ITER (100-350°C). However, their superior thermal stress behavior is seriously compromised by their increasingly poor ductility with increasing temperature above 250°C.

Table 3. Thermal stress figures of merit for high-strength, high conductivity copper alloys

Alloy	M at 20°C (kW/m)	M at 300°C (kW/m)
GlidCop Al25 (IG0)	36	25
CuCrZr (ITER SAA)	32	28
Hycon 3HP CuNiBe (AT)	45	44
Hycon 3HP CuNiBe (HT1)	60	54
Hycon 3HP CuNiBe (HT2)	56	49

The uniform elongation, yield strength and ultimate tensile strength increased with increasing strain rate for all of the alloys tested in this study. This simultaneous improvement in ductility and strength with increasing strain rate is a common feature in face-centered cubic metals, and may be contrasted with the decrease in ductility with increasing strain rate that occurs in body-centered cubic metals [10]. The strain rate sensitivity parameter is defined as [7]

$$m = \frac{1}{\sigma} \frac{\partial \sigma}{\partial \ln \dot{\epsilon}} \quad (1)$$

Several phenomenological models have been developed which describe the combined effects of strain rate and test temperature on deformation behavior in metals. One of the earliest models [11,12] noted that most tensile data obtained on face centered cubic metals at low temperatures (below the creep regime) could be described by a "mechanical equation of state". Although it is generally recognized that a generalized mechanical equation of state cannot be formulated due to temperature-dependent changes in the deformation microstructure, the Zener-Hollomon model is useful for investigating strain rate sensitivity effects. The Zener-Hollomon parameter (P) is given by

$$P = \dot{\epsilon} e^{Q/kT} \quad (2)$$

where $\dot{\epsilon}$ is the strain rate and Q is an activation enthalpy for deformation. It was empirically noted that the flow stress was related to the Zener-Hollomon parameter by a simple power-law exponent [11]. From equation 1, it can be seen that this exponent is the strain rate sensitivity parameter, i.e. $\sigma = P^m$. A similar relation between strain rate and test temperature has been used for analyzing high temperature creep behavior in metals, and is known as the Sherby-Dorn equation [9,13].

$$\left(\frac{\sigma}{E} \right)^n = \frac{\dot{\epsilon}}{A} e^{Q/kT} \quad (3)$$

where E is the temperature-dependent Young's modulus and n and A are constants. It can be readily seen that the stress exponent for the creep equation is simply the reciprocal of the strain rate sensitivity parameter, $n=1/m$. More sophisticated models have been forwarded in recent years which provide a better fit to experimental data, particularly near the threshold stress for creep initiation [14,15]. However, the key strain rate and temperature dependence is still reasonably approximated by eqns 1-3.

Figure 4 compares the yield strength versus reciprocal test temperature for the four copper alloy heats at a strain rate of 1 to $2 \times 10^{-3} \text{ s}^{-1}$. All of the yield strength data have been normalized by the elastic modulus ratio $E' = E(T)/E(20^\circ\text{C})$ so that the deformation activation energy can be readily obtained. A distinct change in slope occurs in all of the alloy curves at a temperature of $\sim 300^\circ\text{C}$, which corresponds to a homologous temperature of $0.42 T_M$ where T_M is the melting temperature. GlidCop exhibited a somewhat higher slope in the low-temperature regime compared to the other alloys, which according to eqns 1-3 may be attributable to its higher strain rate sensitivity parameter m . The deformation activation energy determined from the low-temperature region of the curves in Fig. 4 was $\sim 0.25 \text{ eV}$ for all of the alloys. There were not sufficient data at temperatures above 300°C to accurately determine the deformation activation energy in the high-temperature regime. Analysis of the asymptotic slope obtained from the two highest temperature data points for the different alloys indicated that the high temperature activation energy was comparable to the copper self diffusion energy of 2.07 eV . This suggests that creep is the primary deformation mechanism in the tensile tests performed above 300°C .

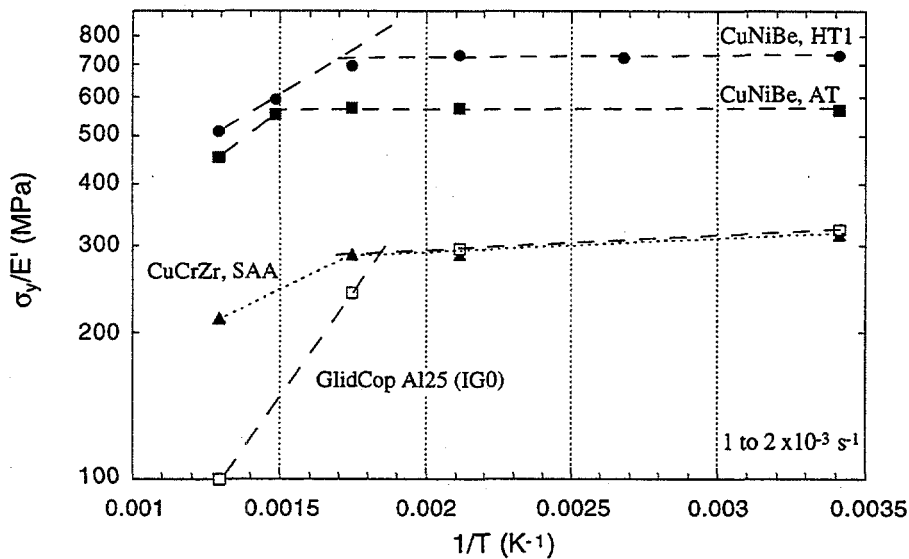


Fig. 4. Comparison of the temperature-dependent yield strengths of the four high-strength, high-conductivity copper alloy heats (normalized by elastic modulus ratio $E' = E(T)/E(20^\circ\text{C})$).

The present results demonstrate that GlidCop Al25 dispersion strengthened copper, CuNiBe and CuCrZr each exhibit different deformation behavior at elevated temperatures. The GlidCop Al25 and the two CuNiBe alloys exhibited significant reductions in uniform elongation with increasing temperature, whereas CuCrZr maintained high uniform elongation levels (>10%) up to 500°C (Table 1). The reduction in uniform elongation at elevated temperatures in the GlidCop Al25 and CuNiBe alloys was particularly severe at low strain rates. Previous tensile studies on wrought GlidCop Al15 and Al25 plates have observed a similar reduction in uniform elongation with increasing test temperature [16]. The GlidCop alloys did not exhibit a corresponding drop in total elongation at high temperatures, indicating that this alloy maintains good ductility in the necked region. On the other hand, the total elongation in the CuNiBe alloys decreased rapidly with increasing test temperature and the fracture mode changed from ductile transgranular failure at room temperature to ductile intergranular failure at temperatures above 300°C [4].

The solutionized and aged CuCrZr specimens were relatively insensitive to strain rate effects, and exhibited only a moderate decrease in strength and elongation with increasing temperature. There is some evidence that Zr additions can inhibit the intermediate temperature embrittlement that is sometimes observed in copper alloys [17-19]. The suppression of embrittlement in Zr-bearing copper alloys has been attributed to either trapping of surface-active bulk impurities such as sulfur [17,18] or else scavenging of atmospheric oxygen at grain boundaries [19]. However, it should be noted that a previous tensile property study on cold-worked and aged Elbrodur CuCrZr (produced by the same vendor as the present study) found low uniform elongations (<1%) and intergranular cracking for test temperatures between 300 and 700°C [20]. Further work is needed to determine the physical mechanisms responsible for low ductility in copper alloys at elevated temperatures.

Recent fracture toughness measurements on GlidCop Al15 and Al25 specimens have found that the fracture toughness decreases rapidly with increasing test temperature between 20 and 250°C [3,21,22]. However, Charpy impact tests of GlidCop Al25 did not show a decrease in absorbed energy for test temperatures up to 350°C [3,21]. The present results suggest that strain rate effects may be partially

responsible for this difference between the static fracture toughness tests ($\sim 10^{-5} \text{ s}^{-1}$) and the Charpy impact tests ($\sim 10 \text{ s}^{-1}$). The tensile strength and ductility of the GlidCop specimens would be significantly lower for the slow strain rates representative of static fracture toughness tests, particularly at elevated temperatures due to the increase in the strain rate sensitivity parameters (m and m'). Possible effects of testing environment (oxygen chemisorption) on the static fracture toughness test results also cannot be discounted, particularly since testing in vacuum at 150-250°C produced about a 50% increase in the measured fracture toughness of Al15 compared to air tests [21,22]. Since 0.5 monolayer of chemisorbed oxygen can reduce the surface energy of pure copper by about a factor of 2 and for copper this oxygen coverage occurs within $\sim 500 \text{ s}$ at a pressure of 10^{-9} torr [23], the partial pressure of oxygen should be less than $\sim 10^{-9}$ torr in order to avoid oxygen effects in the static fracture toughness tests. It is worth noting that the typical oxygen partial pressure between pulses in present-day tokamaks is $\sim 10^{-8}$ to 10^{-7} torr.

Finally, it must be noted that neutron irradiation at ITER-relevant temperatures of 100-250°C would produce significant increases in the strength and decreases in the ductility of these copper alloys [1,2,4]. Unfortunately, relatively little is known about the strain rate sensitivity of neutron irradiated copper alloys. Tensile testing of neutron irradiated specimens at several strain rates and test temperatures (up to the irradiation temperature) should be performed to increase the scientific understanding of deformation processes in radiation hardened copper alloys.

ACKNOWLEDGEMENTS

The GlidCop Al25 plate and Hycon 3HP™ CuNiBe solutionized and aged (AT) specimens for this study were provided by D. J. Edwards, Pacific Northwest National Lab. The two Hycon 3HP™ CuNiBe HT plates were supplied by David Krus, Brush-Wellman, Inc. The CuCrZr plate was supplied in the F37 temper condition by K. Slattery, McDonnell-Douglas.

REFERENCES

- [1] S. J. Zinkle and S. A. Fabritsiev, Atomic and Plasma-Material Interaction Data for Fusion (supplement to Nuclear Fusion) 5 (1994) 163; also Fusion Materials Semiannual Progress Report for period ending March 31, 1994, DOE/ER-0313/16, pp. 314-341.
- [2] S. A. Fabritsiev, S. J. Zinkle, and B. N. Singh, J. Nucl. Mater. 233-237 (1996), 127.
- [3] R. R. Solomon, J. D. Troxell, and A. V. Nadkarni, J. Nucl. Mater. 233-237 (1996), 542.
- [4] S. J. Zinkle and W. S. Eatherly, in Fusion Materials Semiannual Progress Report for Period ending June 30, 1996, DOE/ER-0313/20 (Oak Ridge National Lab, 1996), p. 207.
- [5] D. J. Edwards et al., in Fusion Materials Semiannual Progress Report for Period ending Dec. 31, 1995, DOE/ER-0313/19 (Oak Ridge National Lab, 1996), p. 165.
- [6] G. E. Dieter, Mechanical Metallurgy, 2nd ed (McGraw-Hill, New York, 1976), p. 348.
- [7] P. Haasen, Physical Metallurgy (Cambridge Univ. Press, New York, 1978), p. 26.
- [8] T. P. Blair, personal communication from Westmoreland Mechanical Testing and Research, Inc., Youngstown, PA, to J. W. Davis, McDonnell-Douglas, Oct. 1996.
- [9] J. J. Stephens, R. J. Bourcier, F. J. Vigil, and D.T. Schmale, Sandia National Lab Report SAND88-1351 (1988).
- [10] A. N. Gubbi, A. F. Rowcliffe, W. S. Eatherly, and L.T. Gibson, in Fusion Materials Semiannual Progress Report for Period ending June 30, 1996, DOE/ER-0313/20 (Oak Ridge National Lab, 1996), p. 38.
- [11] C. Zener and J. H. Hollomon, J. Appl. Phys. 15 (1944), 22.
- [12] C. Zener and J. H. Hollomon, J. Appl. Phys. 17 (1946), 69.
- [13] O. D. Sherby and A. K. Miller, J. Engineering Mater. Technology 101 (1979), 387.
- [14] J. Rösler and E. Artz, Acta Metall. 38 (1990), 671.
- [15] J. Groza, J. Mater. Engineering and Performance 1 (1992), 113.
- [16] S. J. Zinkle, S. A. Fabritsiev, B. N. Singh, and D. J. Edwards, J. Nucl. Mater. (1997), to be submitted.

- [17] M. Kanno, *Z. Metallkde.* 79 (1988), 684.
- [18] R.D.K. Misra, V. S. Prasad, and P. R. Rao, *Scripta Mater.* 35 (1996), 129.
- [19] P. Muthiah, A. Guha, and C.J. McMahon, Jr., *Mater. Sci. Forum* 207-209 (1996), 585.
- [20] G. Piatti and D. Boerman, *J. Nucl. Mater.* 185 (1991), 29.
- [21] D. J. Alexander, in *Fusion Materials Semiannual Progress Report for Period ending June 30, 1996*, DOE/ER-0313/20 (ORNL, 1996), p. 217.
- [22] D. J. Alexander, S. J. Zinkle, and A. F. Rowcliffe in *Fusion Materials Semiannual Progress Report for Period ending Dec. 31, 1996*, DOE/ER-0313/21 (Oak Ridge National Lab, 1996), this report.
- [23] S. J. Zinkle and E. H. Lee, *Metall. Trans. A* 21 (1990), 1037.